Appl. Phys. B 52, 245–250 (1991)

Applied Physics B Photophysics and Laser Chemistry

Kinetic Study of a Short-Pulse Electron-Beam Pumped Kr/F_2 Laser Amplifier Medium at Very Low Pressure Operation

Young-Woo Lee and Akira Endoh

Max-Planck-Institut für biophysikalische Chemie, Abteilung Laserphysik, W-3400 Göttingen, Fed. Rep. Germany

Received 21 December 1990/Accepted 7 January 1991

Abstract. A numerical investigation has been performed for very low pressure ($\leq$ 200 Torr) buffer-free KrF laser-amplifier medium pumped by a short pulse (10 ns FWHM) electron beam with low excitation rate operation (200 kW/cm^3). The small-signal-gain coefficient (g_0) and absorption coefficient (α) have been estimated for this new operational mode. The formation and quenching processes are also discussed kinetically.

PACS: 42.55Gp, 42.60By

Recently, the high-power sub-picosecond KrF laser systems [1–5] have been considered as an excellent driving laser for X-ray laser pumping. A peak power of 4 TW was obtained by amplifying a 390 fs pulse to an energy of 1.5 J in three discharge-pumped KrF amplifiers and an electron beam (e-beam) pumped KrF amplifier [4]. In order to realize an X-ray laser excited by a high-intensity petawatt (PW) KrF laser pulse of sub-picosecond pulse duration, the SIMBA (Superhigh Intensity Mono-Beam Amplifier chain) system [6] was recently proposed by the X-ray laser group at the Department of Laser Physics in the Max-Planck-Institut für biophysikalische Chemie. According to the conceptual design of the SIMBA system, the output energy is expected to be 100 J at a pulse duration of 100 fs. A double-pass optical arrangement is assumed in both the preamplifier and the final amplifier in the SIMBA system with single-pass small-signal stage gains of 10 ($g_0L = 2.3$). From the maximum achievable fluence of $3 \times E_{sat}$ (E_{sat}: saturation energy), a clear square aperture of 1.5 m×1.5 m (effective area: 1.3 m×1.3 m) in the final amplifier is required for 100 J output energy with the maximum fluence at the exit window of 6 mJ/cm^2. The length of the pumped region is assumed to be 1.5 m which is the same as the side length of the active aperture. The small-signal-gain coefficient of 1.5%/cm is necessary for this geometry. In order to obtain this short-pulse petawatt laser, the use of an e-beam device is essential for the uniform pumping of a large volume KrF amplifier because of its small saturation energy.

There are two typical operational modes which have been investigated for high-efficiency and high-power e-beam pumped KrF laser amplifier. One is the use of a relatively high pressure laser medium ($\geq$ 1 atm) pumped by a short e-beam pulse ($\leq$ 100 ns FWHM) with a high-excitation-rate pumping scheme ($\geq$ 1 MW/cm^3) [7, 8]. The other is with a long pulse ($\geq$ 200 ns) and low excitation rate ($<$ 200 kW/cm^3) pumping scheme for the angular multiplexing optical system [9, 10]. The e-beam pumped wide aperture KrF laser with a low aspect ratio configuration has been considered as the final high-energy extraction amplifier system for the ICF (Inertial Confinement Fusion) energy driver with reduced Amplified Spontaneous Emission (ASE) to obtain large total energy extraction [11, 12]. In the large amplifier module, in order to solve the problem of window material availability caused by the pressure difference between the laser chamber inside and outside, the atmospheric pressure operation of Kr-rich KrF laser amplifier has been studied experimentally [13]. However, the optimum operational mode for sub-picosecond ultra-high-intensity KrF laser amplifier may be very different from the high energy extraction system for ICF. In the case of ultra-short pulse amplification, the nonlinear processes in the window material are a serious problem [14]. Additionally, the prepulse originating from the ASE in KrF laser amplifier chain causes undesirable plasma formation on the X-ray target before the arrival of the main laser pulse. Shaw and Key [15] have recently suggested a new operational scheme of very low pressure and short pulse e-beam excitation to overcome these problems. Hirst and Shaw [16] measured the net small signal gain as a function of partial Kr gas pressure (gas mixture: $He/Kr/F_2$=8.9/90.6/0.5 (%)) using very low pressure below 150 Torr with a 60 ns (FWHM) e-beam pulse (SPRITE). They obtained the required net small signal gain in excess of 1%/cm readily at 0.1 atm pressure. This experimental result strongly suggests the

possibility of the use of very thin window material to reduce the nonlinear effect under very low pressure condition ($\leq$ 200 Torr) since the laser beam from the final amplifier will be guided to the X-ray target chamber through a vacuum pipe to preserve the beam quality.

In this paper, therefore, we have investigated short-pulse (10 ns FWHM) e-beam pumped low-pressure (< 200 Torr) Kr/F_2 laser medium theoretically. The estimations of small-signal-gain coefficient and absorption coefficient as a function of total pressure and current density have been performed and a kinetic analysis has also been made.

1. Modelling

The numerical procedure and rate constants used are almost the same as reported by Kannari et al. [17] and Lee et al. [18].

We have used 52 chemical reactions for the Kr/F_2 mixture. Two assumptions have been made considering the formation of the KrF upper state. First, the vibrational relaxation of the excited KrF^* state is dependent on the two-body collisional rate with Kr gas using a rate constant [17] of 5×10^{-11} cm^3/s. Second, the B and C states for KrF^* are treated as a single collisional mixing state on the assumptions of a fast B–C mixing process and negligible energy gap [19] of E_B–$E_C = 80\,\text{cm}^{-1}$ and only the low vibrational levels ($v = 0, 1, 2$) of the B state are available for the laser transition. According to the calculated emission rates from low vibrational states of $KrF^*(B)$ [20], we have ignored the contribution of the vibrational states over $v = 3$ whose spectrum is relatively far apart from the center frequencies of $v = 0, 1, 2$. Even at a low total pressure of 30 Torr, the B–C mixing speed is about 1.4 ns when using a Kr/F_2 mixture under the assumption of a collisional mixing rate constant of 5×10^{-10} cm^3/s for Kr [17]. The B–C mixing is still a faster process than other collisional quenching processes at a total pressure of 30 Torr without strong intra-cavity laser intensity. However, if one regards this low-pressure regime for a multipass amplifier, it must be considered that the slow gain recovery time may be caused by the slow vibrational relaxation time (about 20 ns for 30 Torr Kr gas) and relatively slow B–C mixing rate due to the decrease of Kr concentration.

The densities of the rare-gas ions and metastable atoms were calculated by dividing the e-beam deposition energy by the W value [21] of 24.0 eV/ion for Kr.

We also adopted an effective lifetime τ_{eff} for spontaneous emission of the $KrF^*(B, C)$, which is given by

$$1/\tau_{\text{eff}} = \theta_B/\tau_B + \theta_C/\tau_C, \tag{1}$$

where τ_B and τ_C are the spontaneous lifetimes of B and C states, respectively. If the B–C mixing is very fast, the Boltzmann distribution between both B and C states can be assumed. The statistical weight factors θ_B and θ_C are then determined by

$$\theta_B = [1 + \exp(-\Delta E/kT)]^{-1}, \tag{2}$$

$$\theta_C = 1 - \theta_B, \tag{3}$$

where T is the background gas temperature which strongly depends on both the pumping rate and the gas mixture/pressure while $\Delta E = 80\,\text{cm}^{-1}$ is the energy gap of E_B–E_C. As mentioned above, if the rate of B–C mixing is faster than that of the spontaneous radiative emission and collisional relaxation, we can treat the upper state of $KrF^*(B, C)$ as a steady-state equilibrium condition. Consequently, the effective stimulated emission cross section is to be approximately half the value for accessible number density in KrF^*.

On the other hand, the precise multilevel coherent and incoherent interaction model [22] predicted that the saturation energy and small-signal-gain are dependent on the applied laser-pulse width. This is so even if a much shorter pulse width is used than the KrF upper level lifetime which is due to the repumping process of the population in the higher vibrational levels and the mismatching between applied pulse and gain spectrum for the very short pulse regime (< 500 fs). Although we did not consider these effects in this study, it is necessary to investigate the reduction processes in the very short pulse regime experimentally.

The adjustment of collisional quenching rate constants using effective radiative lifetimes was also performed.

2. Results and Discussion

Figure 1 shows a comparison of the net small signal gain as a function of Kr partial pressure pumped by a 60 ns (FWHM) e-beam pulse by using the present kinetic model with the experimental results reported by the Rutherford group [16].

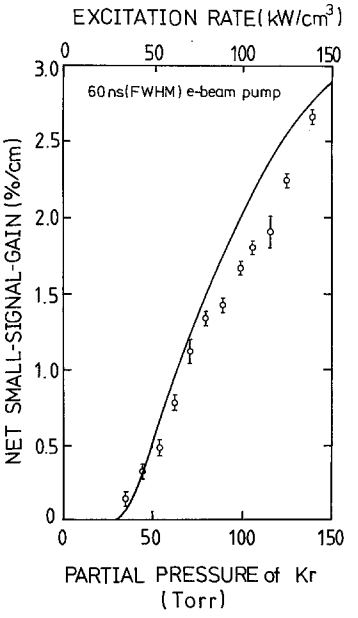

Fig. 1. Comparison of the predicted net small-signal-gains with the experimental results as a function of partial pressure of Kr. The measured excitation rates [16] corresponding to the partial Kr pressure are also shown. The F_2 concentration is kept at 0.5%. The pulse width of e-beam is 60 ns FWHM. The solid curve is the calculated result

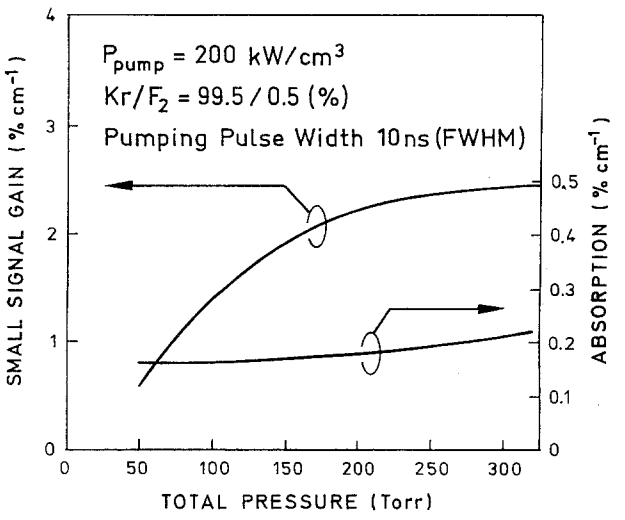

Fig. 2. Calculated peak small-signal-gain coefficient and absorption coefficient versus operational pressure at a constant pump power of 200 kW/cm³. The gas mixture is $KrF/_2$=99.5/0.5 [%]. The pumping pulse width is 10 ns FWHM

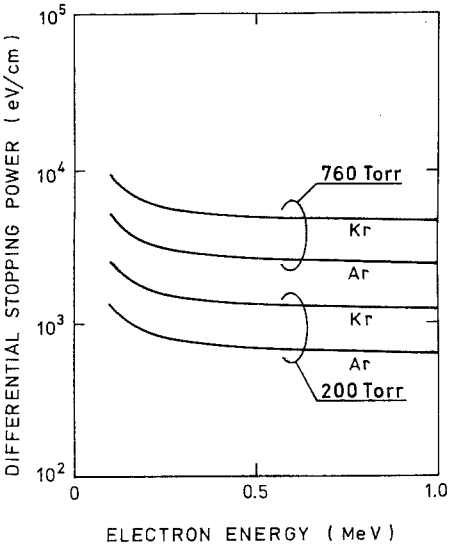

Fig. 3. Stopping powers of Ar and Kr gases as a function of electron energy at pressures of 760 and 200 Torr estimated from the tables of energy losses and ranges of electrons and positrons tabulated by Berger and Seltzer [23]

Our numerical result shows good agreement with the experimental result even in the low-pressure region down to 30 Torr. Our model also predicts the disappearence of net small signal gain below a total pressure of 30 Torr. Possible explanations for this substantial decrease of net small signal gain below a total pressure of 50 Torr are that the formation rate in this low pressure region may be reduced substantially due to the decrease of Kr and F_2 number densities in which Kr is the third body in the main formation process of ion-ion recombination reaction ($Kr^+ + F^- + Kr \rightarrow KrF^* + Kr$) at the low-pressure regime and Kr is also the two-body collisional partner of vibrational relaxation. As a result, the small-signal gain decreases to almost the same value as the absorption of 0.12%/cm at the total pressure of 30 Torr. The absorption coefficients in this pressure region from 30 to 76 Torr are almost a constant value (0.12%/cm at 30 Torr and 0.15%/cm at 76 Torr) in contrast to the fast decrease of small-signal gain.

As noted previously, a short pumping pulse (10 ns FWHM) operating condition is important for an ultra-high-power (PW) amplifier system to improve the system efficiency and the energy contrast ratio (amplified beam intensity/ASE intensity) on the X-ray target. Therefore, our theoretical results presented in the following sections of this paper are calculated under a 10 ns (FWHM) pumping condition. We only investigated Kr/F_2 gas mixtures for obtaining higher specific deposition energy in the low-pressure regime because the e-beam stopping power of Kr gas is a factor of 1.9 times larger than that of Ar gas.

In the SIMBA KrF laser system [6], the driving e-beam diode voltage for the final amplifier is to be 1 MV with a pulsewidth of 10 ns (FWHM). Figure 2 shows the estimated small signal gain and absorption in a mixture of Kr/F_2=99.5/0.5 [%] as a function of the total pressure ranging from 50 to 300 Torr at a constant excitation rate of 200 kW/cm³. The excitation rate of 200 kW/cm³ for the low pressure Kr/F_2 mixture ranging from 50 to 200 Torr within the practical current density region (peak current density of 70 A/cm² for 200 Torr and 280 A/cm² for 50 Torr) is enough for obtaining the expected small-signal gain of 1.5%/cm for the final amplifier of the SIMBA KrF laser system. This limited value is estimated from both the calculated stopping power as a function of electron energy, as shown in Fig. 3, and the conceptual design for the PAM [24] (Power Amplifier Modules) of Los Alamos using 1 MV (20 A/cm²) e-beam pumping scheme with total pressure of 585 Torr which gives an excitation rate of 250 kW/cm³. At the pressure range between 100 and 200 Torr, the small-signal-gains of 1.4–2.2%/cm are to be expected. Here, we used a constant value of 0.5% fluorine as a halogen donor for our very low pressure regime. It is very important to know the optimized fluorine concentration because it is a very important factor in the KrF^* formation and absorption process and the determination of secondary electron number density in the low pressure regime. For a short pulse (10 ns) and low excitation rate ($\leq$ 200 kW/cm³) pumping condition, since the fuel (F_2) burn-up is expected to be a very small quantity, as will be discussed in the following section, we just determined the optimum F_2 concentration which gives the maximum ratio of small-signal gain to absorption (g_0/α). Figure 4 depicts the estimated small-signal gain, absorption, and the ratios of small-signal gain to absorption (g_0/α) and nonsaturable absorption (g_0/α_{ns}) for various total pressure (100–200 Torr) as a function of F_2 concentration at a constant excitation rate of 200 kW/cm³. These values are determined at the time of small-signal-gain peak. The nonsaturable absorption is estimated by

$$\alpha_{ns} = \alpha - \sigma_0 N_{Kr_2F^*}, \tag{4}$$

where α is the absorption (nonsaturable absorption + saturable absorption) and α_{ns} is the nonsaturable absorption, σ_0 is the absorption cross section of Kr_2F^* at

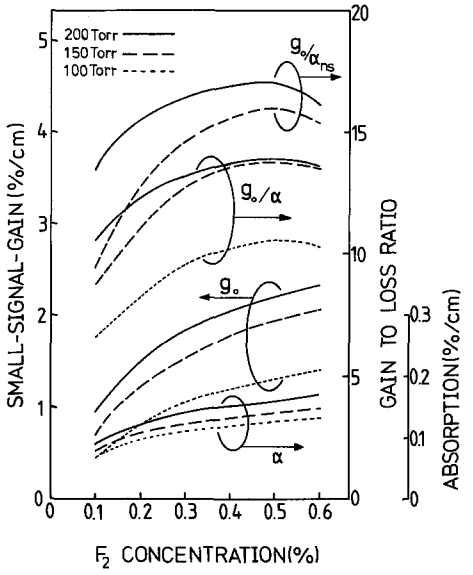

Fig. 4. Calculated small-signal-gain coefficient and absorption coefficient versus F_2 concentration at various total pressures at a constant excitation rate of 200 kW/cm^3. Calculated gain-to-loss ratio (g_0/α) and gain-to-nonsaturable loss ratio (g_0/α_{ns}) as a function of F_2 concentration are also shown

248 nm using the value [25] of 1.6×10^{-18} cm^2 and $N_{Kr_2F^*}$ is the number density. The peak values of g_0/α and g_0/α_{ns} under short pulse (10 ns FWHM) and constant pumping rate (200 kW/cm^3) conditions lie at a F_2 concentration of 0.5% for this low-pressure range (100–200 Torr). The small-signal gain decreases faster than the absorption below 0.5% F_2 due to the decrease of KrF^* formation rate. The ratios of g_0/α for both total pressures of 150 and 200 Torr are almost same value of 13.8 at 0.5% F_2, but the ratio of g_0/α_{ns} for 200 Torr is increasing to 16.8 in contrast to 15.8 for 150 Torr. This increase is mainly due to the increased formation of Kr_2F^* by three-body collisional quenching process ($KrF^*+2\,Kr\rightarrow Kr_2F^*+Kr$) at 200 Torr. Of course, there is another pathway to produce Kr_2F^* by the process [26] of $Kr_2^*+F_2\rightarrow Kr_2F^*+F$ which is a nonsaturable absorber. However, in the low-pressure regime Kr_2F^* is expected to be produced predominantly by three-body collisional quenching of KrF^* because Kr^* forms KrF^* predominantly under the low Kr density condition rather than Kr_2^* which is formed by $Kr^*+2\,Kr$. We assumed all Kr_2F^* are to be a saturable absorber. However, strictly speaking, the Kr_2F^* is not to be a saturable absorber in the case of short-pulse amplification due to the long lifetime [26] of Kr_2F^* in the order of 185 ± 20 ns. From this point of view the g_0/α of 13.8 is more meaningful than the g_0/α_{ns} of 16.8 at the pressure of 200 Torr in the short-pulse (100 fs) amplifier system SIMBA.

Figure 5 displays the temporal evolution of the small-signal gain for various total pressures under the conditions of constant excitation rate of 200 kW/cm^3 with a short-pulse (10 ns FWHM) pumping scheme. At the leading part of the small-signal-gain profile the decrease of formation rate at lower-pressure regime gives rise to a significant delay of peak gain appearance from the peak time of pump pulse (e.g., delay time of about 30 ns for 100 Torr) due to the effects of slower three-body ionic recombination reaction for KrF^* formation and the slower vibrational relaxation time at the lower Kr gas density. These formation processes compete with the electron quenching process during the pump pulse. Figure 6 shows the calculated temporal variation of the selected species for Kr/F_2 (99.5/0.5 [%], 200 Torr) medium pumped by a 10 ns (FWHM) e-beam pulse. The electron number density decreases substantially down to 10^{13} cm^{-3} at the end of e-beam pump pulse which leads to a decrease of electron quenching so that it is negligible at the tail of the small signal gain. As already shown in Fig. 5, the temporal narrowing for higher-pressure regime is mainly due to the increase of collisional quenching by 2 Kr and F_2, and possible explanation for the slow decay rate of small-signal gain at lower-pressure regime is that the reactions such as $Kr^+ + F^- + Kr \rightarrow KrF^* + Kr$ and $Kr^* + F_2 \rightarrow KrF^* + F$ are continuing after the short pump pulse due to the long lifetime of species like Kr^* and Kr^+. In addition, the collisional quenching processes have no significant effects on the latter decay part of small signal gain at the total pressures below 100 Torr which leads to a lifetime of KrF^* that is close to its effective lifetime defined in (1).

In the SIMBA system, the final amplifier will consist of several pumped and unpumped regions. This configuration may cause change of the refractive index in the laser amplifier medium due to the effects of F_2 burn-up and difference of absorption, which lead to the decrease of amplified beam quality. However, the F_2 burn-up is very small, less than 6% during the e-beam pulse (Fig. 6) and the effect of Kr_2F^* absorption is much lower

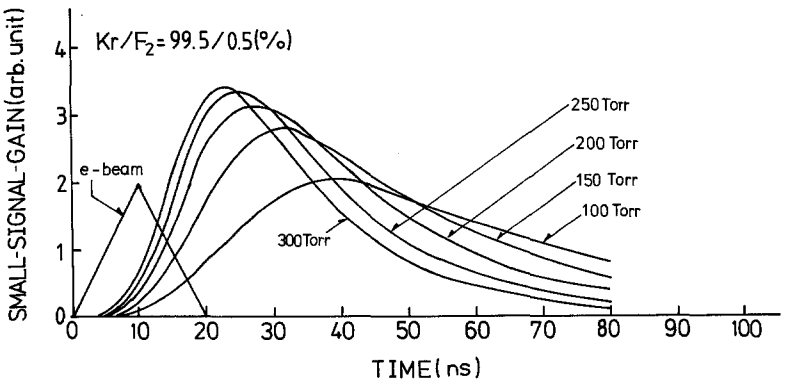

Fig. 5. Calculated temporal variations of the small-signal-gain profile at various total pressures excited by a 10 ns (FWHM) e-beam pulse. The gas mixture is Kr/F_2=99.5/0.5 [%]. The excitation rate is kept constant at 200 kW/cm^3

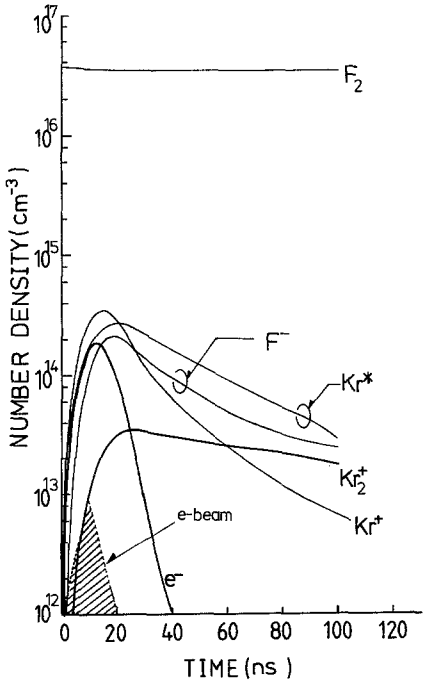

Fig. 6. Calculated temporal variations of selected species for KrF_2 (99.5/0.5 [%]) medium pumped by a short pulse (10 ns FWHM) e-beam with an excitation rate of 200 kW/cm^3

than that expected in conventional atmospheric Kr/F_2 mixture. This is what would be expected because the low pressure below 200 Torr and the short-pulse (10 ns FWHM) e-beam scheme reduce the rate of dissociative attachment and three-body collisional quenching. This indicates that the problem of refractive index change in the Kr/F_2 medium may be neglected in the condition of low pressure and short pulse e-beam with low excitation rate.

Figure 7 shows the estimated temporal variations of formation (a), relaxation (b) and absorption (c) channels under the same condition as in Fig. 6. The formation through ion-ion recombination reactions are a dominant channel (> 60%) in the time scale. The percentage contribution of the neutral formation channel Kr^*+F_2 increases with time due to the long lifetime of Kr^* and the relative decrease of F^- density which also affects the decrease of the absorption channel by F^-. Absorption by F^- and F_2 dominates over 80% of all absorption channels at the time of small-signal-gain peak. Increase of the absorption by Kr_2F^* with time is just due to the relative decrease of F^- density deduced from the percentage contribution of three body collisional quenching by 2 Kr which has an almost constant value of about 15%, as shown in Fig. 7b.

For optimized operation of an e-beam pumped large aperture low-pressure amplifier module, it is necessary to know the current density dependence of gain. Figure 8 shows the calculated small-signal gain as a function of the total pressure (≤ 200 Torr) for current densities 20, 40, 70, and 140 A/cm^2. Since electron number density is proportional to the ratio of the ionization rate to the F_2 density, the F_2 concentration is held at a constant fraction of 0.5% in the calculation which gives constant electron

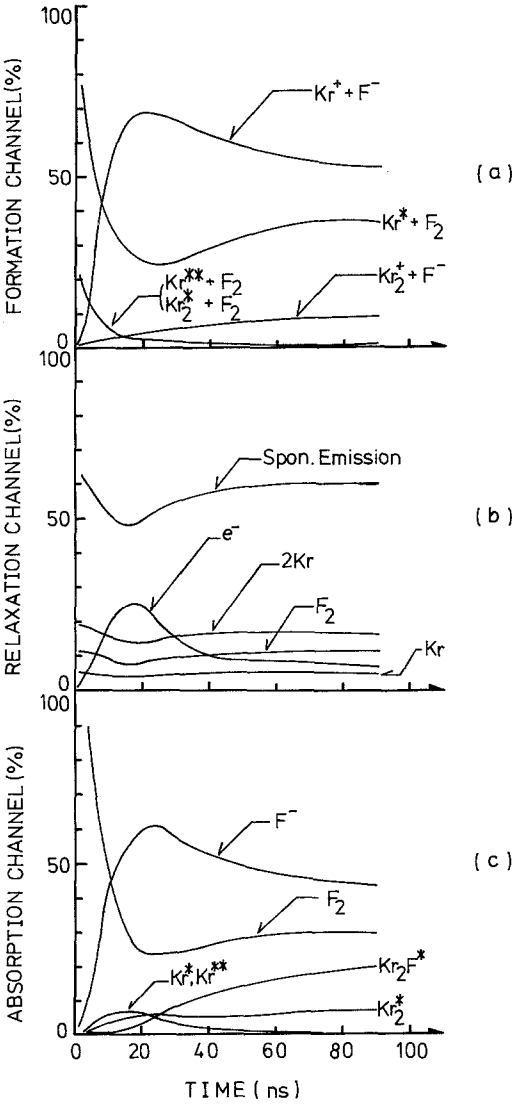

Fig. 7a–c. Calculated temporal dependence of the percent contributions of each component in the KrF^* formation channel (**a**), relaxation channel (**b**), and absorption channel (**c**) under the same condition as in Fig. 6

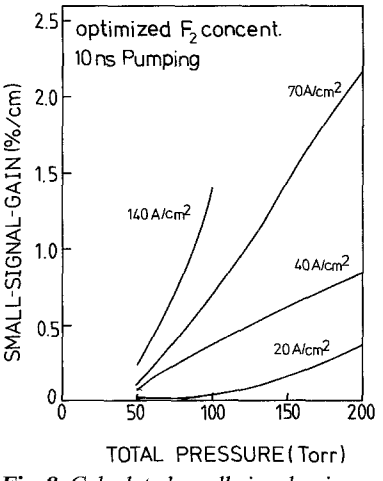

Fig. 8. Calculated small-signal-gain coefficient versus total pressure for various electron-beam current densities. The F_2 concentration is optimized at each current density to maximize g_0/α. The optimum F_2 concentration was 0.5% for all cases in this study

number densities for the total pressure variations. This is so because the excitation rate is simply in proportion to the total pressure with the same mixture condition under the same current density. Even at a current density of $70\,A/cm^2$ for the total pressure range from 150 to 200 Torr, a small-signal gain coefficient of $> 1.5\%/cm$ is obtainable.

3. Conclusion

Very low pressure operation of a short pulse (10 ns) e-beam pumped KrF laser media using Kr/F_2 mixture was studied theoretically because this new operational mode can reduce the optical constraints on a large aperture laser amplifier module in a PW (100 J/100 fs) laser system as an X-ray target driver. The gas kinetics study shows that a small-signal gain of $> 1.5\%/cm$ is obtainable with a high g_0/α of > 11 with the total gas pressure ranging from 150 to 200 Torr pumped by a 10 ns e-beam with the pump rate of $200\,kW/cm^3$. In the low pressure Kr/F_2 mixture with low pump power and short-pulse operation regime, the code calculation predicts the electron quenching and the three-body collisional quenching by 2 Kr is of relatively minor importance. However, the electron quenching process competes with the relatively slow KrF^* formation process during the e-beam pulse. The principal absorbers in this regime are F^- and F_2. This indicates that the increase of F_2 density in the low-pressure regime causes apparently a corresponding increase in absorption even though it has favorable effects, such as reducing the electron quenching and increasing the formation rate. Optimized F_2 concentration of 0.5% in the low-pressure ($\leq$ 200 Torr) Kr/F_2 mixture was estimated by the value which gives the highest g_0/α.

These numerical results strongly suggest that this new operational mode can be applied to a large module KrF amplifier system such as the SIMBA to produce petawatt (100 J/100 fs) laser pulses.

Acknowledgements. The authors would like to thank Prof. F.P. Schäfer and J. Jethwa for their critical reading and making helpful suggestions of the manuscript. Valuable comments and suggestions of Dr. F. Kannari are gratefully acknowledged. We also would like to thank Dr. M.J. Shaw and Dr. G.J. Hirst for their providing of experimental data and helpful discussions. This work was supported by the „Deutsche Forschungsgemeinschaft" by the „Gottfried-Wilhelm-Leibnitz-Programm".

References

1. A.P. Schwarzenbach, T.S. Luk, I.A. McIntyre, U. Johann, A. McPherson, K. Boyer, C.K. Rhodes: Opt. Lett. **11**, 499 (1986)
2. S. Szatmári, F.P. Schäfer, W. Mückenheim, E. Müller-Horsche: Opt. Commun. **63**, 305 (1987)
3. J.P. Roberts, A.J. Taylor, P.H.Y. Lee, R.B. Gibson: Opt. Lett. **13**, 734 (1988)
4. A. Endoh, M. Watanabe, N. Sarukura, S. Watanabe: Opt. Lett. **14**, 353 (1989)
5. C.H. Nam, W. Tighe, E. Valeo, S. Suckewer: Appl. Phys. B **50**, 275 (1990)
6. S. Szatmári, G. Kühnle, A. Endoh, F.P. Schäfer, J. Jasny, Y.W. Lee, J. Jethwa, U. Teubner, G. Kovács: "Technical Proposal for the ELF 100 J/100 fs KrF-Laser System SIMBA", Oct. 1990 (unpublished)
7. C.B. Edwards, F. O'Neill, M.J. Shaw: Appl. Phys. Lett. **36**, 617 (1981)
8. F. Kannari, M. Obara, T. Fujioka: Jpn. J. Appl. Phys. **22**, L 739 (1983)
9. D.D. Lowenthal, J.J. Ewing, R.E. Center, P.B. Mumora, W.M. Grossmann, N.T. Olson, L.P. Shannon: IEEE J. QE-**17**, 1861 (1981)
10. J.J. Ramirez: Proc. 4th IEEE Pulsed Power Conference (IEEE, New York 1983) p. 751
11. G.W. York, Jr., S.J. Czuchlewski, L.A. Rosocha, E.T. Saleski: Digest of Technical Papers, CLEO '85, 188 (1985)
12. D.D. Lowenthal, J.M. Eggleston: IEEE J. QE-**22**, 1165 (1986)
13. A. Suda, H. Kumagai, M. Obara: Appl. Phys. Lett. **51**, 218 (1987)
14. A.J. Taylor, R.B. Gibson, J.P. Roberts: Opt. Lett. **13**, 814 (1988)
15. M.J. Shaw, M.H. Key: Annual Report of RAL-90-026, 202 (1990)
16. G.J. Hirst, M.J. Shaw: To be published in Appl. Phys. B
17. F. Kannari, M. Obara, T. Fujioka: J. Appl. Phys. **57**, 4309 (1985)
18. Y.-W. Lee, F. Kannari, M. Obara: J. Appl. Phys. **65**, 4532 (1989)
19. P.S. Julienne, M. Krauss: Appl. Phys. Lett. **35**, 55 (1979)
20. J.J. Ewing: *Laser Handbook*, ed. by M.L. Stitch (North-Holland, Amsterdam 1979)
21. L.G. Christophorou: *Atomic and Molecular Radiation Physics* (Wiley, New York 1971)
22. F. Kannari: J. Appl. Phys. **67**, 3954 (1990)
23. M.J. Berger, S.M. Seltzer: Nat. Aeronaut. and Space Administration, Washington, DC, Rep. NASA SP-3012 (1964)
24. J.A. Sullivan: Fusion Tech. **11**, 684 (1987)
25. J.H. Schloss, D.B. Geohegan, J.G. Eden: Presented at Int. Laser Sci. Conf., Seattle, WA, Oct. 21–24 (1986)
26. A. Luches, V. Nassisi, A. Perrone, M.R. Perrone: Opt. Commun. **39**, 307 (1981)